
On the Numerical Solution of the Elliptic Monge–Ampère Equation in Dimension Two: A Least-Squares Approach

Edward J. Dean and Roland Glowinski

University of Houston, Department of Mathematics, 651 P. G. Hoffman Hall,
Houston, TX 77204-3008, USA roland@math.uh.edu, dean@math.uh.edu

1 Introduction

During his outstanding career, *Olivier Pironneau* has addressed the solution of a large variety of problems from the Natural Sciences, Engineering and Finance to name a few, an evidence of his activity being the many articles and books he has written. It is the opinion of these authors, and former collaborators of O. Pironneau (cf. [DGP91]), that this chapter is well-suited to a volume honoring him. Indeed, the two pillars of the solution methodology that we are going to describe are: (1) a nonlinear least squares formulation in an appropriate Hilbert space, and (2) a mixed finite element approximation, reminiscent of the one used in [DGP91] and [GP79] for solving the Stokes and Navier–Stokes equations in their stream function–vorticity formulation; the contributions of O. Pironneau on the two above topics are well-known world wide. Last but not least, we will show that the solution method discussed here can be viewed as a solution method for a non-standard variant of the incompressible Navier–Stokes equations, an area where O. Pironneau has many outstanding and celebrated contributions (cf. [Pir89], for example).

The main goal of this article is to discuss the *numerical solution* of the *Dirichlet problem* for the prototypical *two-dimensional elliptic Monge–Ampère equation*, namely

$$\det \mathbf{D}^2\psi = f \text{ in } \Omega, \quad \psi = g \text{ on } \Gamma. \quad (\text{E-MA-D})$$

In (E-MA-D): (1) Ω is a bounded domain of \mathbb{R}^2 and Γ is its boundary; (2) f and g are given functions with $f > 0$; $\mathbf{D}^2\psi = (\partial^2\psi/\partial x_i\partial x_j)_{1\leq i,j\leq 2}$ is the *Hessian* of the unknown function ψ . The partial differential equation in (E-MA-D) is a *fully nonlinear elliptic* one (in the sense of, e.g., Gilbarg and Trudinger [GT01] and Caffarelli and Cabré [CC95]). The *mathematical analysis* of problems such as (E-MA-D) has produced a quite abundant literature; let us mention, among many others, [GT01, CC95, Aub82, Aub98, Cab02] and the references therein. On the other hand, and to the best of our knowledge, the *numerical analysis* community has largely ignored these problems,

so far, some notable exceptions being provided by [BB00, OP88, CKO99] (see also [DG03, DG04]). Indeed we can not resist quoting [BB00] (an article dedicated to the numerical solution of the celebrated *Monge–Kantorovitch optimal transportation problem*):

“It follows from this theoretical result that a natural computational solution of the L2 MKP is the numerical resolution of the Monge–Ampère equation (6). Unfortunately, this fully nonlinear second-order elliptic equation has not received much attention from numerical analysts and, to the best of our knowledge, there is no efficient finite-difference or finite-element methods, comparable to those developed for linear second-order elliptic equations (such as fast Poisson solvers, multigrid methods, preconditioned conjugate gradient methods, . . .).”

We will show in this article that, actually, fully nonlinear elliptic problems such as (E-MA-D) can be solved by appropriate combinations of fast Poisson solvers and preconditioned conjugate gradient methods. However, unlike the (*closely related*) Dirichlet problem for the Laplace operator, the problem (E-MA-D) may have *multiple solutions* (actually, two at most; cf., e.g., [CH89, Chapter 4]), and the *smoothness* of the data does not imply the existence of a smooth solution. Concerning the last property, suppose that $\Omega = (0, 1) \times (0, 1)$ and consider the special case where (E-MA-D) is defined by

$$\frac{\partial^2 \psi}{\partial x_1^2} \frac{\partial^2 \psi}{\partial x_2^2} - \left| \frac{\partial^2 \psi}{\partial x_1 \partial x_2} \right|^2 = 1 \quad \text{in } \Omega, \quad \psi = 0 \quad \text{on } \Gamma. \quad (1)$$

The problem (1) can not have smooth solutions since, for those solutions, the boundary condition $\psi = 0$ on Γ implies that the product $(\partial^2 \psi / \partial x_1^2)(\partial^2 \psi / \partial x_2^2)$ and the cross-derivative $\partial^2 \psi / \partial x_1 \partial x_2$ vanish at the boundary, implying in turn that $\det \mathbf{D}^2 \psi$ is strictly less than one in some neighborhood of Γ . The above (non-existence) result is not a consequence of the non-smoothness of Γ , since a similar non-existence property holds if in (1) one replaces the above Ω by the ovoid-shaped domain whose C^∞ -boundary is defined by

$$\Gamma = \bigcup_{i=1}^4 \Gamma_i,$$

with

$$\begin{aligned} \Gamma_1 &= \{x \mid x = \{x_1, x_2\}, x_2 = 0, 0 \leq x_1 \leq 1\}, \\ \Gamma_3 &= \{x \mid x = \{x_1, x_2\}, x_2 = 1, 0 \leq x_1 \leq 1\}, \\ \Gamma_2 &= \{x \mid x = \{x_1, x_2\}, x_1 = 1 - \ln 4 / (\ln x_2 (1 - x_2)), 0 \leq x_2 \leq 1\}, \\ \Gamma_4 &= \{x \mid x = \{x_1, x_2\}, x_1 = \ln 4 / (\ln x_2 (1 - x_2)), 0 \leq x_2 \leq 1\}. \end{aligned}$$

Actually, for the above two Ω s the non-existence of solutions for the problem (1) follows from the *non-strict convexity* of these domains. Albeit the problem

(1) has no classical solution it has *viscosity solutions* in the sense of Crandall–Lions, as shown in, e.g., [CC95, Cab02, Jan88, Urb88, CIL92]. The Crandall–Lions viscosity approach relies heavily on the *maximum principle*, unlike the *variational methods* used to solve, for example, the second order linear elliptic equations in divergence form in some appropriate subspace of the Hilbert space $H^1(\Omega)$. The *least-squares* approach discussed in this article operates in the space $H^2(\Omega) \times \mathbf{Q}$ where \mathbf{Q} is the Hilbert space of the 2×2 symmetric tensor-valued functions with component in $L^2(\Omega)$. Combined with *mixed finite element approximations* and *operator-splitting methods* it will have the ability, if g has the $H^{3/2}(\Gamma)$ -regularity, to capture classical solutions, if such solutions exist, and to compute *generalized solutions* to problems like (1) which have no classical solution. Actually, we will show that these generalized solutions are also *viscosity solutions*, but in a sense different from Crandall–Lions’.

Remark 1. Suppose that Ω is simply connected. Let us define a vector-valued function \mathbf{u} by $\mathbf{u} = \left\{ \frac{\partial \psi}{\partial x_2}, -\frac{\partial \psi}{\partial x_1} \right\}$ ($= \{u_1, u_2\}$). The problem (E-MA-D) takes then the equivalent formulation

$$\begin{cases} \det \nabla \mathbf{u} = f & \text{in } \Omega, \quad \nabla \cdot \mathbf{u} = 0 \text{ in } \Omega, \\ \mathbf{u} \cdot \mathbf{n} = \frac{dg}{ds} & \text{on } \Gamma, \end{cases} \quad (2)$$

where \mathbf{n} denotes the outward unit vector normal at Γ , and s is a counter-clockwise curvilinear abscissa. Once \mathbf{u} is known, one obtains ψ via the solution of the following Poisson–Dirichlet problem:

$$-\Delta \psi = \frac{\partial u_2}{\partial x_1} - \frac{\partial u_1}{\partial x_2} \quad \text{in } \Omega, \quad \psi = g \quad \text{on } \Gamma.$$

The problem (2) has clearly an *incompressible fluid flow flavor*, ψ playing here the role of a *stream function*. The relations (2) can be used to solve the problem (E-MA-D) but this approach will not be further investigated here.

Remark 2. As shown in [DG05], the methodology discussed in this article applies also (among other problems) to the *Pucci–Dirichlet problem*

$$\alpha \lambda^+ + \lambda^- = 0 \quad \text{in } \Omega, \quad \psi = g \quad \text{on } \Gamma, \quad (\text{PUC-D})$$

with λ^+ (resp., λ^-) the *largest* (resp., the *smallest*) *eigenvalue* of $\mathbf{D}^2 \psi$ and $\alpha \in (1, +\infty)$. (If $\alpha = 1$, one recovers the linear Poisson–Dirichlet problem.)

Remark 3. A shortened version of this article can be found in [DG04].

Remark 4. The solution of (E-MA-D) by *augmented Lagrangian methods* is discussed in [DG03, DG06a, DG06b].

2 A Least Squares Formulation of the Problem (E-MA-D)

From now on, we suppose that $f > 0$ and that $\{f, g\} \in \{L^1(\Omega), H^{3/2}(\Gamma)\}$, implying that the following space and set are *non-empty*:

$$V_g = \{\varphi \mid \varphi \in H^2(\Omega), \varphi = g \text{ on } \partial\Omega\},$$

$$\mathbf{Q}_f = \{\mathbf{q} \mid \mathbf{q} \in \mathbf{Q}, \det \mathbf{q} = f\},$$

with

$$\mathbf{Q} = \{\mathbf{q} \mid \mathbf{q} \in (L^2(\Omega))^{2 \times 2}, \mathbf{q} = \mathbf{q}^t\}.$$

Solving the Monge–Ampère equation in $H^2(\Omega)$ is equivalent to looking for the intersection in \mathbf{Q} of the two sets \mathbf{D}^2V_g and \mathbf{Q}_f , an infinite dimensional geometry problem “visualized” in Figures 1 and 2.

If $\mathbf{D}^2V_g \cap \mathbf{Q}_f \neq \emptyset$ as “shown” in Figure 1, then the problem (E-MA-D) has a solution in $H^2(\Omega)$. If, on the other hand, it is the situation of Figure 2 which prevails, namely $\mathbf{D}^2V_g \cap \mathbf{Q}_f = \emptyset$, (E-MA-D) has no solution in $H^2(\Omega)$. However, Figure 2 is *constructive* in the sense that it suggests looking for a pair $\{\psi, \mathbf{p}\}$ which *minimizes*, globally or locally, some distance between $\mathbf{D}^2\varphi$ and \mathbf{q} when $\{\varphi, \mathbf{q}\}$ describes the set $V_g \times \mathbf{Q}_f$.

According to the above suggestion, and in order to handle those situations where (E-MA-D) has no solution in $H^2(\Omega)$, despite the fact that neither V_g nor \mathbf{Q}_f are empty, we suggest to solve the above problem via the following (nonlinear) *least squares formulation*:

$$\begin{cases} \text{Find } \{\psi, \mathbf{p}\} \in V_g \times \mathbf{Q}_f \text{ such that} \\ j(\psi, \mathbf{p}) \leq j(\varphi, \mathbf{q}), \forall \{\varphi, \mathbf{q}\} \in V_g \times \mathbf{Q}_f, \end{cases} \quad \text{(LSQ)}$$

where, in (LSQ) and below, we have (with $dx = dx_1 dx_2$):

$$j(\varphi, \mathbf{q}) = \frac{1}{2} \int_{\Omega} |\mathbf{D}^2\varphi - \mathbf{q}|^2 dx \quad (3)$$

and

$$|\mathbf{q}| = (q_{11}^2 + q_{22}^2 + 2q_{12}^2)^{1/2}, \quad \forall \mathbf{q} = (q_{ij})_{1 \leq i, j \leq 2} \in \mathbf{Q}. \quad (4)$$

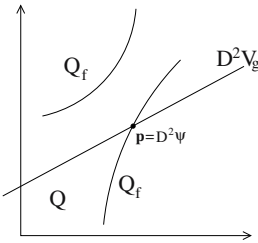


Fig. 1. Problem (E-MA-D) has a solution in $H^2(\Omega)$.

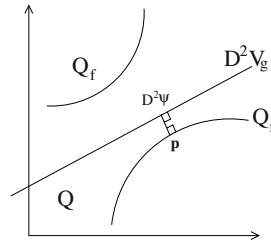


Fig. 2. Problem (E-MA-D) has no solution in $H^2(\Omega)$.

Remark 5. The results (described in [DG05]), concerning the numerical solution of the Pucci’s problem (PUC-D) (see Remark 2), suggest that defining $|\mathbf{q}|$ by

$$|\mathbf{q}| = (q_{11}^2 + q_{22}^2 + q_{12}^2)^{1/2}, \quad \forall \mathbf{q} = (q_{ij})_{1 \leq i, j \leq 2} \in \mathbf{Q}, \quad (5)$$

instead of (4), may improve the convergence of the algorithms to be described in the following sections. We intend to check this conjecture in a near future.

In order to solve (LSQ) by *operator-splitting techniques* it is convenient to observe that (LSQ) is *equivalent* to

$$\begin{cases} \{\psi, \mathbf{p}\} \in V_g \times \mathbf{Q}, \\ j_f(\psi, \mathbf{p}) \leq j_f(\varphi, \mathbf{q}), \quad \forall \{\varphi, \mathbf{q}\} \in V_g \times \mathbf{Q}, \end{cases} \quad (\text{LSQ-P})$$

where

$$j_f(\varphi, \mathbf{q}) = j(\varphi, \mathbf{q}) + I_f(\mathbf{q}), \quad \forall \{\varphi, \mathbf{q}\} \in V_g \times \mathbf{Q}, \quad (6)$$

with

$$I_f(\mathbf{q}) = \begin{cases} 0, & \text{if } \mathbf{q} \in \mathbf{Q}_f, \\ +\infty, & \text{if } \mathbf{q} \in \mathbf{Q} \setminus \mathbf{Q}_f, \end{cases}$$

i.e., $I_f(\cdot)$ is the *indicator functional* of the set \mathbf{Q}_f .

3 An Operator-Splitting Based Method for the Solution of (E-MA-D) via (LSQ-P)

We can solve the least-squares problem (LSQ) by a *block relaxation method* operating *alternatively* between V_g and \mathbf{Q}_f . Such relaxation algorithms are discussed in, e.g., [Glo84]. Closely related algorithms are obtained as follows:

- Step 1. Derive the *Euler-Lagrange equation* of (LSQ-P).
- Step 2. Associate to the above *Euler-Lagrange equation* an *initial value problem* (flow in the Dynamical System terminology) in $V_g \times \mathbf{Q}$.
- Step 3. Use *operator-splitting* to time discretize the above flow problem.

Applying the above program, Step 1 provides us with the *Euler–Lagrange equation* of the problem (LSQ-P). A *variational formulation* of this equation reads as follows:

$$\begin{cases} \{\psi, \mathbf{p}\} \in V_g \times \mathbf{Q}, \\ \int_{\Omega} (\mathbf{D}^2\psi - \mathbf{p}) : (\mathbf{D}^2\varphi - \mathbf{q}) \, dx + \langle \partial I_f(\mathbf{p}), \mathbf{q} \rangle = 0, \quad \forall \{\varphi, \mathbf{q}\} \in V_0 \times \mathbf{Q}, \end{cases} \quad (7)$$

where $\partial I_f(\mathbf{p})$ denotes a *generalized differential* of the functional $I_f(\cdot)$ at \mathbf{p} . Next, we have denoted by $\mathbf{S} : \mathbf{T}$ the *Fröbenius scalar product* of the two 2×2 symmetric tensors $\mathbf{S} (= (s_{ij}))$ and $\mathbf{T} (= (t_{ij}))$, namely

$$\mathbf{S} : \mathbf{T} = s_{11}t_{11} + s_{22}t_{22} + 2s_{12}t_{12}$$

and, finally,

$$V_0 = H^2(\Omega) \cap H_0^1(\Omega).$$

Next, we achieve Step 2 by associating with (7) the following *initial value problem* (flow), written in *semi-variational form*:

$$\left\{ \begin{array}{l} \text{Find } \{\psi(t), \mathbf{p}(t)\} \in V_g \times \mathbf{Q} \text{ for all } t > 0 \text{ such that} \\ \int_{\Omega} [\partial(\Delta\psi)/\partial t] \Delta\varphi \, dx + \int_{\Omega} \mathbf{D}^2\psi : \mathbf{D}^2\varphi \, dx = \int_{\Omega} \mathbf{p} : \mathbf{D}^2\varphi \, dx, \quad \forall \varphi \in V_0, \\ \partial\mathbf{p}/\partial t + \mathbf{p} + \partial I_f(\mathbf{p}) = \mathbf{D}^2\psi, \\ \{\psi(0), \mathbf{p}(0)\} = \{\psi_0, \mathbf{p}_0\}, \end{array} \right. \quad (8)$$

and we look at the limit of $\{\psi(t), \mathbf{p}(t)\}$ as $t \rightarrow +\infty$. The choice of ψ^0 and \mathbf{p}^0 will be discussed in Remark 6.

Finally, concerning Step 3 we advocate the following *operator-splitting scheme* (à la *Marchuk–Yanenko*, see, e.g., [Glo03, Chapter 6] and the references therein), but we acknowledge that other splitting schemes are possible:

$$\{\psi^0, \mathbf{p}^0\} = \{\psi_0, \mathbf{p}_0\}. \quad (9)$$

Then, for $n \geq 0$, $\{\psi^n, \mathbf{p}^n\}$ being known, we obtain $\{\psi^{n+1}, \mathbf{p}^{n+1}\}$ from the solution of

$$\begin{array}{l} (\mathbf{p}^{n+1} - \mathbf{p}^n)/\tau + \mathbf{p}^{n+1} + \partial I_f(\mathbf{p}^{n+1}) = \mathbf{D}^2\psi^n, \\ \left\{ \begin{array}{l} \psi^{n+1} \in V_g; \\ \int_{\Omega} \Delta [(\psi^{n+1} - \psi^n)/\tau] \Delta\varphi \, dx + \int_{\Omega} \mathbf{D}^2\psi^{n+1} : \mathbf{D}^2\varphi \, dx = \\ = \int_{\Omega} \mathbf{p}^{n+1} : \mathbf{D}^2\varphi \, dx, \quad \forall \varphi \in V_0; \end{array} \right. \end{array} \quad (10)$$

above, $\tau (> 0)$ is a *time-discretization step*.

The solution of the sub-problems (10) and (11) will be discussed in Sections 4 and 5, respectively.

Remark 6. The initialization of the flow defined by (8) and of its time-discrete variant defined by (9)–(11) are clearly important issues. Let us denote by λ_1 and λ_2 the *eigenvalues* of the Hessian $\mathbf{D}^2\psi$. It follows from (E-MA-D) that $\lambda_1\lambda_2 = f$, implying in turn that

$$\sqrt{\lambda_1\lambda_2} = \sqrt{f}. \quad (12)$$

We have, on the other hand,

$$|\Delta\psi| = |\lambda_1 + \lambda_2|. \quad (13)$$

Suppose that we look for a *convex solution* of (E-MA-D). We have then λ_1 and λ_2 positive. Comparing (12) (geometric mean) and (13) (arithmetic mean) suggests to define ψ_0 as the solution of

$$\Delta\psi_0 = 2\sqrt{f} \quad \text{in } \Omega, \quad \psi_0 = g \quad \text{on } \Gamma. \tag{14}$$

If we look for a *concave solution* we suggest to define ψ_0 as the solution of

$$-\Delta\psi_0 = 2\sqrt{f} \quad \text{in } \Omega, \quad \psi_0 = g \quad \text{on } \Gamma. \tag{15}$$

If $\{f, g\} \in L^1(\Omega) \times H^{3/2}(\Gamma)$, then $\{\sqrt{f}, g\} \in L^2(\Omega) \times H^{3/2}(\Gamma)$, implying that each of the problems (14) and (15) has a unique solution in V_g (assuming of course that Ω is convex and/or that Γ is sufficiently smooth). Concerning \mathbf{p}^0 an obvious choice is provided by

$$\mathbf{p}_0 = \mathbf{D}^2\psi_0, \tag{16}$$

another possibility being

$$\mathbf{p}_0 = \begin{pmatrix} \sqrt{f} & 0 \\ 0 & \sqrt{f} \end{pmatrix}. \tag{17}$$

The symmetric tensor defined by (17) belongs clearly to \mathbf{Q}_f .

4 On the Solution of the Nonlinear Sub-Problems (10)

Concerning the solution of the sub-problems of type (10), we interpret (10) as the *Euler–Lagrange* equation of the following minimization problem:

$$\begin{cases} \mathbf{p}^{n+1} \in \mathbf{Q}_f, \\ J_n(\mathbf{p}^{n+1}) \leq J_n(\mathbf{q}), \quad \forall \mathbf{q} \in \mathbf{Q}_f, \end{cases} \tag{18}$$

with

$$J_n(\mathbf{q}) = \frac{1}{2}(1 + \tau) \int_{\Omega} |\mathbf{q}|^2 dx - \int_{\Omega} (\mathbf{p}^n + \tau \mathbf{D}^2\psi^n) : \mathbf{q} dx. \tag{19}$$

It follows from (19) that the problem (18) can be solved point-wise on Ω (in practice, at the grid points of a finite element or finite difference mesh). To be more precise, we have to solve, *a.e.* on Ω , a minimization problem of the following type:

$$\begin{cases} \min_{\mathbf{z}} \left[\frac{1}{2}(z_1^2 + z_2^2 + 2z_3^2) - b_1(x)z_1 - b_2(x)z_2 - 2b_3(x)z_3 \right] \\ \text{with } \mathbf{z} \left(= \{z_i\}_{i=1}^3 \right) \in \{ \mathbf{z} \mid \mathbf{z} \in \mathbb{R}^3, z_1z_2 - z_3^2 = f(x) \}. \end{cases} \tag{20}$$

Actually, if one looks for *convex* (resp., *concave*) *solutions* of (E-MA-D), we should prescribe the following additional constraints: $z_1 \geq 0, z_2 \geq 0$ (resp., $z_1 \leq 0, z_2 \leq 0$). For the solution of the problem (20) (a constrained

minimization problem in R^3) we advocate those methods discussed in, e.g., [DS96] (after introduction of a Lagrange multiplier to handle the constraint $z_1 z_2 - z_3^2 = f(x)$). Other methods are possible, including the reduction of (20) to a two-dimensional problem via the elimination of z_3 . Indeed, we observe that (20) is equivalent to

$$\left\{ \begin{array}{l} \min_{\mathbf{z}} \left[\frac{1}{2} (z_1 + z_2)^2 - b_1(x)z_1 - b_2(x)z_2 - 2|b_3(x)|(z_1 z_2 - f(x))^{\frac{1}{2}} \right] \\ \text{with } \mathbf{z} (= \{z_i\}_{i=1}^3) \in \left\{ \mathbf{z} \mid \mathbf{z} \in \mathbb{R}^3, z_1 z_2 - f(x) \geq 0, \right. \\ \left. z_3 = \text{sgn}(b_3(x))(z_1 z_2 - f(x))^{\frac{1}{2}} \right\}, \end{array} \right. \quad (21)$$

which leads to the above mentioned reduction; then we make “almost” trivial the solution of the problem (21) by using the following change of variables (reminiscent of the polar coordinate based technique used in [DG05] for the solution of the Pucci’s equation (PUC-D), introduced in Remark 2):

$$z_1 = \rho\sqrt{f}e^\theta, \quad z_2 = \rho\sqrt{f}e^{-\theta},$$

with $\theta \in R$ and $\rho \geq 1$ (resp., $\rho \leq -1$) if one looks for a convex (resp., concave) solution of (E-MA-D).

5 On the Conjugate Gradient Solution of the Linear Sub-Problems (11)

The sub-problems (11) are all members of the following family of *linear variational problems*:

$$\left\{ \begin{array}{l} u \in V_g, \\ \int_{\Omega} \Delta u \Delta v \, dx + \tau \int_{\Omega} \mathbf{D}^2 u : \mathbf{D}^2 v \, dx = L(v), \quad \forall v \in V_0, \end{array} \right. \quad (22)$$

with the functional L linear and continuous from $H^2(\Omega)$ into \mathbb{R} ; the problems in (22) are clearly of the *biharmonic* type. The *conjugate gradient* solution of linear variational problems in Hilbert spaces, such as (22), has been addressed in, e.g., [Glo03, Chapter 3]. Following the above reference, we are going to solve (22) by a conjugate gradient algorithm operating in the spaces V_0 and V_g , both spaces being equipped with the scalar product defined by

$$\{v, w\} \rightarrow \int_{\Omega} \Delta v \Delta w \, dx,$$

and the corresponding norm. This conjugate gradient algorithm reads as follows:

Algorithm 1

Step 1. u^0 is given in V_g .

Step 2. Solve then

$$\begin{cases} g^0 \in V_0, \\ \int_{\Omega} \Delta g^0 \Delta v \, dx = \int_{\Omega} \Delta u^0 \Delta v \, dx + \tau \int_{\Omega} \mathbf{D}^2 u^0 : \mathbf{D}^2 v \, dx - L(v), \\ \forall v \in V_0, \end{cases} \quad (23)$$

and set $w^0 = g^0$.

Step 3. Then, for $k \geq 0$, u^k, g^k, w^k being known, the last two different from 0, we compute u^{k+1}, g^{k+1} , and if necessary w^{k+1} , as follows:

Solve

$$\begin{cases} \bar{g}^k \in V_0, \\ \int_{\Omega} \Delta \bar{g}^k \Delta v \, dx = \int_{\Omega} \Delta w^k \Delta v \, dx + \tau \int_{\Omega} \mathbf{D}^2 w^k : \mathbf{D}^2 v \, dx, \\ \forall v \in V_0, \end{cases} \quad (24)$$

and compute

$$\rho_k = \frac{\int_{\Omega} |\Delta g^k|^2 \, dx}{\int_{\Omega} \Delta \bar{g}^k \Delta w^k \, dx}, \quad (25)$$

$$u^{k+1} = u^k - \rho_k w^k, \quad (26)$$

$$g^{k+1} = g^k - \rho_k \bar{g}^k. \quad (27)$$

Step 4. If $\int_{\Omega} |\Delta g^{k+1}|^2 \, dx / \int_{\Omega} |\Delta g^0|^2 \, dx \leq \text{tol}$ take $u = u^{k+1}$; else, compute

$$\gamma_k = \frac{\int_{\Omega} |\Delta g^{k+1}|^2 \, dx}{\int_{\Omega} |\Delta g^k|^2 \, dx} \quad (28)$$

and

$$w^{k+1} = g^{k+1} + \gamma_k w^k. \quad (29)$$

Step 5. Do $k = k + 1$ and return to Step 3.

Numerical experiments have shown that Algorithm 1 (in fact, its discrete variants) has excellent convergence properties when applied to the solution of (E-MA-D). Combined with an appropriate mixed finite element approximation of (E-MA-D) it requires the solution of two discrete Poisson problems at each iteration.

6 On a Mixed Finite Element Approximation of the Problem (E-MA-D)

6.1 Generalities

Considering the highly *variational* flavor of the methodology discussed in Sections 2 to 5, it makes sense to look for *finite element* based methods for the approximation of (E-MA-D). In order to avoid the complications associated to the construction of finite element subspaces of $H^2(\Omega)$, we will employ a *mixed finite element approximation* (closely related to those discussed in, e.g., [DGP91, GP79] for the solution of linear and nonlinear *biharmonic* problems). Following this approach, it will be possible to solve (E-MA-D) employing approximations commonly used for the solution of the second order elliptic problems (piecewise linear and globally continuous over a triangulation of Ω , for example).

6.2 A Mixed Finite Element Approximation

For simplicity, we suppose that Ω is a bounded polygonal domain of \mathbb{R}^2 . Let us denote by \mathcal{T}_h a *finite element triangulation* of Ω (like those discussed in, e.g., [Glo84, Appendix 1]). From \mathcal{T}_h we approximate spaces $L^2(\Omega)$, $H^1(\Omega)$ and $H^2(\Omega)$ by the finite dimensional space V_h defined by

$$V_h = \{v \mid v \in C^0(\bar{\Omega}), v|_T \in P_1, \forall T \in \mathcal{T}_h\}, \quad (30)$$

with P_1 the space of the two-variable polynomials of degree ≤ 1 . A function φ being given in $H^2(\Omega)$ we denote $\frac{\partial^2 \varphi}{\partial x_i \partial x_j}$ by $D_{ij}^2(\varphi)$. It follows from *Green's formula* that

$$\int_{\Omega} \frac{\partial^2 \varphi}{\partial x_i^2} v \, dx = - \int_{\Omega} \frac{\partial \varphi}{\partial x_i} \frac{\partial v}{\partial x_i} \, dx, \quad \forall v \in H_0^1(\Omega), \quad \forall i = 1, 2, \quad (31)$$

$$\int_{\Omega} \frac{\partial^2 \varphi}{\partial x_1 \partial x_2} v \, dx = - \frac{1}{2} \int_{\Omega} \left[\frac{\partial \varphi}{\partial x_1} \frac{\partial v}{\partial x_2} + \frac{\partial \varphi}{\partial x_2} \frac{\partial v}{\partial x_1} \right] \, dx, \quad \forall v \in H_0^1(\Omega). \quad (32)$$

Consider now $\varphi \in V_h$. Taking advantage of the relations (31) and (32), we define the discrete analogues of the differential operators D_{ij}^2 by

$$\begin{cases} \forall i = 1, 2, & D_{hii}^2(\varphi) \in V_{0h}, \\ \int_{\Omega} D_{hii}^2(\varphi) v \, dx = - \int_{\Omega} \frac{\partial \varphi}{\partial x_i} \frac{\partial v}{\partial x_i} \, dx, & \forall v \in V_{0h}, \end{cases} \quad (33)$$

$$\begin{cases} D_{h12}^2(\varphi) \in V_{0h}, \\ \int_{\Omega} D_{h12}^2(\varphi) v \, dx = - \frac{1}{2} \int_{\Omega} \left[\frac{\partial \varphi}{\partial x_1} \frac{\partial v}{\partial x_2} + \frac{\partial \varphi}{\partial x_2} \frac{\partial v}{\partial x_1} \right] \, dx, & \forall v \in V_{0h}, \end{cases} \quad (34)$$

where the space V_{0h} is defined by

$$V_{0h} = V_h \cap H_0^1(\Omega) (= \{v \mid v \in V_h, v = 0 \text{ on } \Gamma\}). \quad (35)$$

The functions $D_{hij}^2(\Omega)$ are *uniquely* defined by the relations (33) and (34). However, in order to simplify the computation of the above discrete second order partial derivatives we will use the *trapezoidal rule* to evaluate the integrals in the left hand sides of (33) and (34). Owing to their practical importance, let us detail these calculations:

1. First we introduce the set Σ_h of the vertices of \mathcal{T}_h and then $\Sigma_{0h} = \{P \mid P \in \Sigma_h, P \notin \Gamma\}$. Next, we define the integers N_h and N_{0h} by $N_h = \text{Card}(\Sigma_h)$ and $N_{0h} = \text{Card}(\Sigma_{0h})$. We have then $\dim V_h = N_h$ and $\dim V_{0h} = N_{0h}$. We suppose that $\Sigma_{0h} = \{P_k\}_{k=1}^{N_{0h}}$ and $\Sigma_h = \Sigma_{0h} \cup \{P_k\}_{k=N_{0h}+1}^{N_h}$.
2. To $P_k \in \Sigma_h$ we associate the function w_k *uniquely* defined by

$$w_k \in V_h, \quad w_k(P_k) = 1, \quad w_k(P_l) = 0, \quad \text{if } l = 1, \dots, N_h, \quad l \neq k. \quad (36)$$

It is well known (see, e.g., [Glo84, Appendix 1]) that the sets $\mathcal{B}_h = \{w_k\}_{k=1}^{N_h}$ and $\mathcal{B}_{0h} = \{w_k\}_{k=1}^{N_{0h}}$ are *vector bases* of V_h and V_{0h} , respectively.

3. Let us denote by A_k the area of the polygonal which is the union of those triangles of \mathcal{T}_h which have P_k as a common vertex. Applying the trapezoidal rule to the integrals in the left hand side of the relations (33) and (34), we obtain:

$$\begin{cases} \forall i = 1, 2, \quad D_{hii}^2(\varphi) \in V_{0h}, \\ D_{hii}^2(\varphi)(P_k) = -\frac{3}{A_k} \int_{\Omega} \frac{\partial \varphi}{\partial x_i} \frac{\partial w_k}{\partial x_i} dx, \quad \forall k = 1, 2, \dots, N_{0h}, \end{cases} \quad (37)$$

$$\begin{cases} D_{h12}^2(\varphi) (= D_{h21}^2(\varphi)) \in V_{0h}, \\ D_{h12}^2(\varphi)(P_k) = -\frac{3}{2A_k} \int_{\Omega} \left[\frac{\partial \varphi}{\partial x_1} \frac{\partial w_k}{\partial x_2} + \frac{\partial \varphi}{\partial x_2} \frac{\partial w_k}{\partial x_1} \right] dx, \\ \forall k = 1, 2, \dots, N_{0h}. \end{cases} \quad (38)$$

Computing the integrals in the right hand sides of (37) and (38) is quite simple since the first order derivatives of φ and w_k are *piecewise constant*.

Taking the above relations into account, approximating (E-MA-D) is now a fairly simple issue. Assuming that the boundary function g is *continuous* over Γ , we approximate the affine space V_g by

$$V_{gh} = \{\varphi \mid \varphi \in V_h, \varphi(P) = g(P), \forall P \in \Sigma_h \cap \Gamma\}, \quad (39)$$

and then (E-MA-D) by

$$\begin{cases} \text{Find } \psi_h \in V_{gh} \text{ such that for all } k = 1, 2, \dots, N_{0h}, \\ D_{h11}^2(\psi_h)(P_k) D_{h22}^2(\psi_h)(P_k) - |D_{h12}^2(\psi_h)(P_k)|^2 = f_h(P_k). \end{cases} \quad (\text{E-MA-D})_h$$

The *iterative solution* of the problem (E-MA-D)_h will be discussed in the following paragraph.

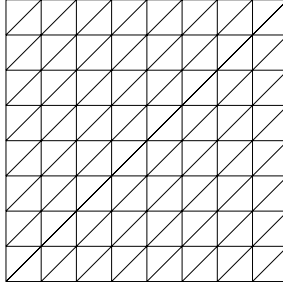


Fig. 3. A uniform triangulation of $\Omega = (0, 1)^2$ ($h = 1/8$)

Remark 7. Suppose that $\Omega = (0, 1)^2$ and that triangulation \mathcal{T}_h is like the one shown in Figure 3.

Suppose that $h = \frac{1}{I+1}$, I being a positive integer greater than 1. In this particular case, the sets Σ_h and Σ_{0h} are given by

$$\begin{cases} \Sigma_h = \{P_{ij} \mid P_{ij} = \{ih, jh\}, 0 \leq i, j \leq I + 1\}, \\ \Sigma_{0h} = \{P_{ij} \mid P_{ij} = \{ih, jh\}, 1 \leq i, j \leq I\}, \end{cases} \quad (40)$$

implying that $N_h = (I + 2)^2$ and $N_{0h} = I^2$. It follows then from the relations (37) and (38) that (with obvious notation):

$$D_{h11}^2(\varphi)(P_{ij}) = \frac{\varphi_{i+1,j} + \varphi_{i-1,j} - 2\varphi_{ij}}{h^2}, \quad 1 \leq i, j \leq I, \quad (41)$$

$$D_{h22}^2(\varphi)(P_{ij}) = \frac{\varphi_{i,j+1} + \varphi_{i,j-1} - 2\varphi_{ij}}{h^2}, \quad 1 \leq i, j \leq I, \quad (42)$$

and

$$\begin{aligned} D_{h12}^2(\varphi)(P_{ij}) &= \frac{(\varphi_{i+1,j+1} + \varphi_{i-1,j-1} + 2\varphi_{ij})}{2h^2} \\ &\quad - (\varphi_{i+1,j} + \varphi_{i-1,j} + \varphi_{i,j+1} + \varphi_{i,j-1}) / (2h^2), \quad 1 \leq i, j \leq I. \end{aligned} \quad (43)$$

The finite difference formulas (41)–(43) are exact for the polynomials of degree ≤ 2 . Also, as expected,

$$D_{h11}^2(\varphi)(P_{ij}) + D_{h22}^2(\varphi)(P_{ij}) = \frac{\varphi_{i+1,j} + \varphi_{i-1,j} + \varphi_{i,j+1} + \varphi_{i,j-1} - 4\varphi_{ij}}{h^2}; \quad (44)$$

we have recovered, thus, the well-known 5-point discretization formula for the finite difference approximation of the Laplace operator.

6.3 On the Least-squares Formulation of (E-MA-D)_h

Inspired by Sections 3 to 5, we will discuss now the solution of (E-MA-D)_h by a discrete variant of the solution methods discussed there. The first step in

this direction is to approximate the least-squares problem (LSQ). To achieve this goal, we approximate the sets \mathbf{Q} and \mathbf{Q}_f by

$$\mathbf{Q}_h = \{\mathbf{q} \mid \mathbf{q} = (q_{ij})_{1 \leq i, j \leq 2}, q_{21} = q_{12}, q_{ij} \in V_{0h}\} \quad (45)$$

and

$$\mathbf{Q}_{fh} = \{\mathbf{q} \mid \mathbf{q} \in \mathbf{Q}_h, q_{11}(P_k)q_{22}(P_k) - |q_{12}(P_k)|^2 = f_h(P_k), \\ \forall k = 1, 2, \dots, N_{0h}\}, \quad (46)$$

respectively, the function f_h in (46) (and in $(\text{E-MA-D})_h$) being a continuous approximation of f . Next, we approximate the *least-squares functional* $j(\cdot, \cdot)$ (defined by (3) in Section 2) by $j_h(\cdot, \cdot)$ defined as follows:

$$j_h(\varphi, \mathbf{q}) = \frac{1}{2} \|\mathbf{D}_h^2 \varphi - \mathbf{q}\|_h^2, \quad \forall \varphi \in V_h, \mathbf{q} \in \mathbf{Q}_h, \quad (47)$$

with

$$\mathbf{D}_h^2 \varphi = (D_{hij}^2(\varphi))_{1 \leq i, j \leq 2}, \quad (48)$$

$$((\mathbf{S}, \mathbf{T}))_h = \frac{1}{3} \sum_{k=1}^{N_{0h}} A_k \mathbf{S}(P_k) : \mathbf{T}(P_k) \\ \left(= \frac{1}{3} \sum_{k=1}^{N_{0h}} A_k (s_{11}t_{11} + s_{22}t_{22} + 2s_{12}t_{12})(P_k) \right), \quad \forall \mathbf{S}, \mathbf{T} \in \mathbf{Q}_h, \quad (49)$$

and then

$$\|\mathbf{S}\|_h = ((\mathbf{S}, \mathbf{S}))_h^{1/2}, \quad \forall \mathbf{S} \in \mathbf{Q}_h. \quad (50)$$

From the above relations, we approximate the problem (LSQ) by the following *discrete least-squares problem*:

$$\begin{cases} \{\psi_h, \mathbf{p}_h\} \in V_{gh} \times \mathbf{Q}_{fh}, \\ j_h(\psi_h, \mathbf{p}_h) \leq j_h(\varphi, \mathbf{q}), \quad \forall \{\varphi, \mathbf{q}\} \in V_{gh} \times \mathbf{Q}_{fh}. \end{cases} \quad (51)$$

6.4 On the Solution of the Problem (51)

To solve the minimization problem (51), we shall use the following discrete variant of the algorithm (9)–(11):

$$\{\psi^0, \mathbf{p}^0\} = \{\psi_0, \mathbf{p}_0\}. \quad (52)$$

Then, for $n \geq 0$, $\{\psi^n, \mathbf{p}^n\}$ being known, compute $\{\psi^{n+1}, \mathbf{p}^{n+1}\}$ via the solution of

$$\mathbf{p}^{n+1} = \arg \min_{\mathbf{q} \in \mathbf{Q}_{fh}} \left[\frac{1}{2} (1 + \tau) \|\mathbf{q}\|_h^2 - ((\mathbf{p}^n + \tau \mathbf{D}_h^2 \psi^n, \mathbf{q}))_h \right], \quad (53)$$

and

$$\begin{cases} \psi^{n+1} \in V_{gh}, \\ (\Delta_h[(\psi^{n+1} - \psi^n)/\tau], \Delta_h \varphi)_h + ((\mathbf{D}_h^2 \psi^{n+1}, \mathbf{D}_h^2 \varphi))_h \\ = ((\mathbf{p}^{n+1}, \mathbf{D}_h^2 \varphi))_h, \quad \forall \varphi \in V_{0h}, \end{cases} \quad (54)$$

where we have

$$(1) \quad \Delta_h \varphi = D_{h11}^2(\varphi) + D_{h22}^2(\varphi), \quad \forall \varphi \in V_h, \quad (55)$$

$$(2) \quad (\varphi_1, \varphi_2)_h = \frac{1}{3} \sum_{k=1}^{N_{0h}} A_k \varphi_1(P_k) \varphi_2(P_k), \quad \forall \varphi_1, \varphi_2 \in V_{0h}, \quad (56)$$

the associated norm being still denoted by $\|\cdot\|_h$.

The constrained minimization sub-problems (53) decompose into N_{0h} three-dimensional minimization problems (one per internal vertex of \mathcal{T}_h) similar to those encountered in Section 4, concerning the solution of the problem (10). The various solution methods (briefly) discussed in Section 4 still apply here. For the solution of the *linear* sub-problems (54), we advocate the following discrete variant of the *conjugate gradient* algorithm (23)–(29) (Algorithm 1):

Algorithm 2

Step 1. u^0 is given in V_{gh} .

Step 2. Solve

$$\begin{cases} g_h^0 \in V_{0h}, \\ (\Delta_h g^0, \Delta_h \varphi)_h = (\Delta_h u^0, \Delta_h \varphi)_h + \tau((\mathbf{D}_h^2 u^0, \mathbf{D}_h^2 \varphi))_h - L_h(\varphi), \\ \quad \forall \varphi \in V_{0h}, \end{cases} \quad (57)$$

and set

$$w^0 = g^0. \quad (58)$$

Step 3. Then, for $k \geq 0$, assuming that u^k, g^k and w^k are known with the last two different from 0, solve

$$\begin{cases} \bar{g}^k \in V_{0h}, \\ (\Delta_h \bar{g}^k, \Delta_h \varphi)_h = (\Delta_h w^k, \Delta_h \varphi)_h + \tau((\mathbf{D}_h^2 w^k, \mathbf{D}_h^2 \varphi))_h, \\ \quad \forall \varphi \in V_{0h}, \end{cases} \quad (59)$$

and compute

$$\rho_k = (\Delta_h g^k, \Delta_h \bar{g}^k)_h / (\Delta_h \bar{g}^k, \Delta_h w^k)_h, \quad (60)$$

$$u^{k+1} = u^k - \rho_k w^k, \quad (61)$$

$$g^{k+1} = g^k - \rho_k \bar{g}^k. \quad (62)$$

Step 4. If $(\Delta_h g^k, \Delta_h g^k)_h / (\Delta_h g^0, \Delta_h g^0)_h \leq \text{tol.}$ take $u = u^{k+1}$; else, compute

$$\gamma_k = (\Delta_h g^{k+1}, \Delta_h g^{k+1})_h / (\Delta_h g^k, \Delta_h g^k)_h \quad (63)$$

and update w^k via

$$w^{k+1} = g^{k+1} + \gamma_k w^k. \quad (64)$$

Step 5. Do $k + 1 \rightarrow k$ and return to Step 3.

When solving the sub-problems (54), the linear functional $L_h(\cdot)$ encountered in (57) reads as follows:

$$L_h(\varphi) = (\Delta_h \psi^n, \Delta_h \varphi)_h + \tau((\mathbf{P}^{n+1}, \mathbf{D}_h^2 \varphi))_h.$$

Concerning the solution of the discrete *bi-harmonic problems* (57) and (59), let us observe that both problems are of the following type:

$$\begin{cases} \text{Find } u_h \in V_{0h} \text{ (or } V_{gh}) \text{ such that} \\ (\Delta_h u_h, \Delta_h v)_h = L_h(v), \quad \forall v \in V_{0h}, \end{cases} \quad (65)$$

the functional $L_h(\cdot)$ being linear. Let us denote $-\Delta_h u_h$ by ω_h . It follows then from (37), (55) and (56) that the problem (65) is equivalent to the following system of two coupled discrete Poisson–Dirichlet problems:

$$\begin{cases} \omega_h \in V_{0h}, \\ \int_{\Omega} \nabla \omega_h \cdot \nabla v \, dx = L_h(v), \quad \forall v \in V_{0h}, \end{cases} \quad (66)$$

$$\begin{cases} u_h \in V_{0h} \text{ (or } V_{gh}), \\ \int_{\Omega} \nabla u_h \cdot \nabla v \, dx = (\omega_h, v)_h, \quad \forall v \in V_{0h}. \end{cases} \quad (67)$$

Both problems are well-posed. Actually, the solution (by direct or iterative methods) of discrete Poisson problems, such as (66) and (67), has motivated an important literature; some related references can be found in [Glo03, Chapter 5].

We shall conclude this section by observing that via the algorithm (52)–(54) we have thus reduced the solution of (E-MA-D) $_h$ to the solution of

1. a sequence of discrete (linear) Poisson–Dirichlet problems.
2. a sequence of minimization problems in \mathbb{R}^3 (or \mathbb{R}^2).

7 Numerical Experiments

The least-squares based methodology discussed in the above sections has been applied to the solution of three particular (E-MA-D) problems, with $\Omega = (0, 1)^2$. The *first test problem* can be formulated as follows (with $|x| = (x_1^2 + x_2^2)^{1/2}$ and $R \geq \sqrt{2}$):

$$\det D^2\psi = \frac{R^2}{(R^2 - |x|^2)^{\frac{1}{2}}} \quad \text{in } \Omega, \quad \psi = (R^2 - |x|^2)^{\frac{1}{2}} \quad \text{on } \Gamma. \quad (68)$$

The function ψ defined by $\psi(x) = (R^2 - |x|^2)^{1/2}$ is a solution to the problem (68). Its graph is a piece of the sphere of center $\mathbf{0}$ and radius R . We have discretized the problem (68) relying on the mixed finite element approximation discussed in Section 6, associated to a uniform triangulation of Ω (like the one shown on Figure 3, but finer). The uniformity of the mesh allows us to solve the various elliptic problems encountered at each iteration of the algorithm (57)–(64) (Algorithm 2) by fast Poisson solvers taking advantage of the decomposition properties of the discrete analogues of the biharmonic problems (23) and (24). To initialize the algorithm (52)–(54), we followed Remark 6 (see Section 3) and defined ψ_0 as the solution of the discrete Poisson problem

$$\begin{cases} \psi_0 \in V_{gh}, \\ \int_{\Omega} \nabla \psi_0 \cdot \nabla v \, dx = 2(\sqrt{f_h}, v)_h, \quad \forall v \in V_{0h} \end{cases}$$

and \mathbf{p}_0 by $\mathbf{p}_0 = \mathbf{D}_h^2 \psi_0$. The algorithm (52)–(54) diverges if $R = \sqrt{2}$ (which is not surprising since the corresponding $\psi \notin H^2(\Omega)$). On the other hand, for $R = 2$ we have a quite fast convergence as soon as τ is large enough, the corresponding results being reported in Table 1. (We stopped iterating as soon as $\|D_h^2 \psi_h^n - \mathbf{p}_h^n\|_{0,\Omega} \leq 10^{-6}$.)

Above, $\{\psi_h^c, \mathbf{p}_h^c\}$ is the computed approximate solution, h the space discretization step, n_{it} the number of iterations necessary to achieve convergence, and $\|D_h^2 \psi_h^c - \mathbf{p}_h^c\|_{0,\Omega}$ is a trapezoidal rule based approximation of

Table 1. First test problem: convergence results

| h | τ | n_{it} | $\ D_h^2 \psi_h^c - \mathbf{p}_h^c\ _{\mathbf{Q}}$ | $\ \psi_h^c - \psi\ _{L^2(\Omega)}$ |
|------|--------|----------|--|-------------------------------------|
| 1/32 | 0.1 | 517 | 0.9813×10^{-6} | 0.450×10^{-5} |
| 1/32 | 1 | 73 | 0.9618×10^{-6} | 0.449×10^{-5} |
| 1/32 | 10 | 28 | 0.7045×10^{-6} | 0.450×10^{-5} |
| 1/32 | 100 | 21 | 0.6773×10^{-6} | 0.449×10^{-5} |
| 1/32 | 1,000 | 22 | 0.8508×10^{-6} | 0.449×10^{-5} |
| 1/32 | 10,000 | 22 | 0.8301×10^{-6} | 0.449×10^{-5} |
| 1/64 | 1 | 76 | 0.9624×10^{-6} | 0.113×10^{-5} |
| 1/64 | 10 | 29 | 0.8547×10^{-6} | 0.113×10^{-5} |
| 1/64 | 100 | 24 | 0.8094×10^{-6} | 0.113×10^{-5} |

$(\int_{\Omega} |\mathbf{D}_h^2 \psi_h^c - \mathbf{p}_h^c|^2 dx)^{1/2}$. Table 1 clearly suggests that: (1) For τ large enough the speed of convergence is essentially independent of τ ; (2) The speed of convergence is essentially independent of h ; (3) The $L^2(\Omega)$ -approximation error is $O(h^2)$.

The *second test problem* is defined by

$$\det \mathbf{D}^2 \psi = \frac{1}{|x|} \quad \text{in } \Omega, \quad \psi = \frac{2\sqrt{2}}{3} |x|^{\frac{3}{2}} \quad \text{on } \Gamma. \tag{69}$$

With these data, the function ψ defined by $\psi(x) = \frac{2\sqrt{2}}{3} |x|^{\frac{3}{2}}$ is a solution of the problem (69). It is easily shown that $\psi \in W^{2,p}(\bar{\Omega})$ for all $p \in [1, 4)$, but does not have the $C^2(\bar{\Omega})$ -regularity. Using the same approximation and algorithms than for the first test problem, we obtain the results reported in Table 2.

The various comments we have done concerning the solution of the first test problem still apply here. The graphs of f and ψ_h^c (for $h = 1/64$) have been visualized in Figures 4 and 5, respectively.

The *third test problem*, namely

$$\det D^2 \psi = 1 \quad \text{in } \Omega, \quad \psi = 0 \quad \text{on } \Gamma, \tag{70}$$

has no solution in $H^2(\Omega)$, despite the smoothness of the data, making it, by far, the more interesting (in some sense) of our test problems, from a computational point of view. We have reported in Table 3 the results produced by the algorithm (52)–(54) using $\|\psi_h^{n+1} - \psi_h^n\|_{L^2(\Omega)} \leq 10^{-7}$ as the stopping criterion.

It is clear from Table 3 that the convergence is slower than for the first two test problems, however, some important features remain such as: the number of iterations necessary to achieve convergence is essentially independent of τ , as soon as this parameter is large enough, and increases slowly with $1/h$ (actually like $h^{-1/2}$). In Figures 6, 7 and 8 we have shown, respectively, the graph of ψ_h^c (for $h = 1/64$), the graph of the function $x_1 \rightarrow \psi_h^c(x_1, 1/2)$ when $x_1 \in [0, 1]$, and the graph of the restriction of ψ_h^c to the line $x_1 = x_2$ (i.e., the

Table 2. Second test problem: convergence results

| h | τ | n_{it} | $\ D_h^2 \psi_h^c - \mathbf{p}_h^c\ _{\mathbf{Q}}$ | $\ \psi_h^c - \psi\ _{L^2(\Omega)}$ |
|------|--------|----------|--|-------------------------------------|
| 1/32 | 1 | 145 | 0.9381×10^{-6} | 0.556×10^{-4} |
| 1/32 | 10 | 56 | 0.9290×10^{-6} | 0.556×10^{-4} |
| 1/32 | 100 | 46 | 0.9285×10^{-6} | 0.556×10^{-4} |
| 1/32 | 1,000 | 45 | 0.9405×10^{-6} | 0.556×10^{-4} |
| 1/64 | 1 | 151 | 0.9500×10^{-6} | 0.145×10^{-4} |
| 1/64 | 10 | 58 | 0.9974×10^{-6} | 0.145×10^{-4} |
| 1/64 | 100 | 49 | 0.9531×10^{-6} | 0.145×10^{-4} |
| 1/64 | 1,000 | 48 | 0.9884×10^{-6} | 0.145×10^{-4} |

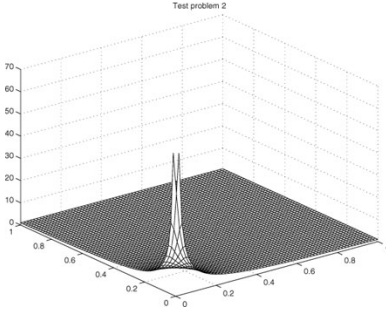


Fig. 4. Second test problem: graph of f .

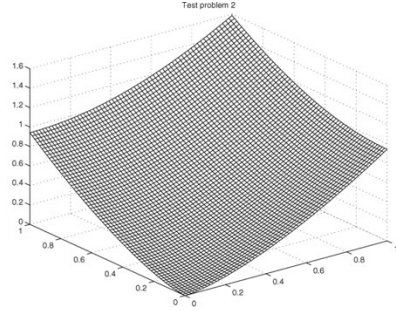


Fig. 5. Second test problem: graph of ψ_h^c ($h = 1/64$)

Table 3. Third test problem: convergence results

| h | τ | n_{it} | $\ D_h^2 \psi_h^c - \mathbf{p}_h^c\ _{\mathbf{Q}}$ |
|-------|--------|----------|--|
| 1/32 | 1 | 4,977 | 0.1054×10^{-1} |
| 1/32 | 100 | 3,297 | 0.4980×10^{-2} |
| 1/32 | 1,000 | 3,275 | 0.4904×10^{-2} |
| 1/32 | 10,000 | 3,273 | 0.4896×10^{-2} |
| 1/64 | 1 | 6,575 | 0.1993×10^{-1} |
| 1/64 | 100 | 4,553 | 0.1321×10^{-1} |
| 1/64 | 1,000 | 4,527 | 0.1312×10^{-1} |
| 1/128 | 100 | 5,401 | 0.1841×10^{-1} |
| 1/128 | 1,000 | 5,372 | 0.1830×10^{-1} |

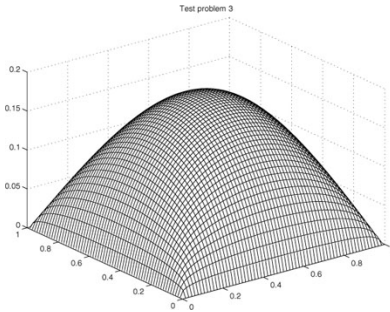


Fig. 6. Third test problem: graph of ψ_h^c ($h = 1/64$)

graph of the function $\xi \rightarrow \psi_h^c(\xi, \xi)$ when $\xi \in [0, 1]$). In Figures 7 and 8, we used $- \cdot - \cdot$ (resp., $- - -$ and $-$) to represent the results corresponding to $h = 1/32$ (resp., $h = 1/64$ and $h = 1/128$).

The results in Figures 7 and 8 suggest strongly that ψ_h converges to a limit as $h \rightarrow 0$. They suggest also that the convergence is *superlinear* with respect to h . The above limit can be viewed as a *generalized solution* of (E-MA-D)

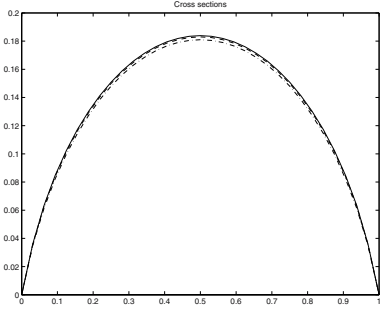


Fig. 7. Third test problem: graph of ψ_h^c restricted to the line $x_2 = 1/2$

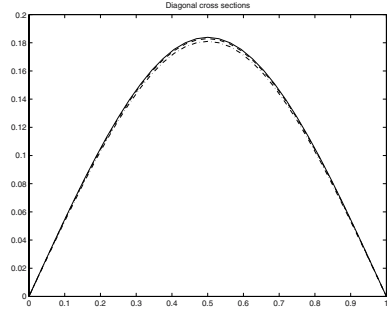


Fig. 8. Third test problem: graph of ψ_h^c restricted to the line $x_1 = x_2$

(in a *least-squares sense*). Actually, a closer inspection of the numerical results shows that the curvature of the graph is negative close to the corners, implying that the Monge–Ampère equation (70) is violated there (since the curvature is given by $\det \mathbf{D}^2\psi / (1 + |\nabla\psi|^2)^2$). Indeed, as expected, it is also violated along the boundary, since $\|\mathbf{D}_h^2\psi_h^c\|_{0,\Omega} \approx 10^{-2}$, while $\|\mathbf{D}_h^2\psi_h^c\|_{0,\Omega_1} \approx 10^{-4}$ and $\|\mathbf{D}_h^2\psi_h^c\|_{0,\Omega_2} \approx 10^{-5}$, where $\Omega_1 = (1/8, 7/8)^2$ and $\Omega_2 = (1/4, 3/4)^2$. These results show that in that particular case, at least, the Monge–Ampère equation $\det \mathbf{D}^2\psi = 1$ is verified with a good accuracy, sufficiently far away from Γ .

8 Further Comments

A natural question arising from the material discussed in the above sections is the following one: *Does our least-squares methodology provide viscosity solutions?*

We claim that indeed the solutions obtained by the least-squares methodology discussed in the preceding sections are (kind of) *viscosity solutions*. To show this property, let us consider (as in Section 3) the *flow* associated with the least-squares optimality conditions (7). We have then

$$\left\{ \begin{array}{l} \text{Find } \{\psi(t), \mathbf{p}(t)\} \in V_g \times \mathbf{Q} \text{ for all } t > 0 \text{ such that} \\ \int_{\Omega} \partial(\Delta\psi)/\partial t \Delta\varphi \, dx + \int_{\Omega} \mathbf{D}^2\psi : \mathbf{D}^2\varphi \, dx \\ \qquad = \int_{\Omega} \mathbf{p} : \mathbf{D}^2\varphi \, dx, \quad \forall \varphi \in V_0, \\ \int_{\Omega} \partial\mathbf{p}/\partial t : \mathbf{q} \, dx + \int_{\Omega} \mathbf{p} : \mathbf{q} \, dx + \langle \partial I_{\mathbf{Q}_f}(\mathbf{p}), \mathbf{q} \rangle \\ \qquad = \int_{\Omega} \mathbf{D}^2\psi : \mathbf{q} \, dx, \quad \forall \mathbf{q} \in \mathbf{Q}, \\ \{\psi(0), \mathbf{p}(0)\} = \{\psi_0, \mathbf{p}_0\}. \end{array} \right. \tag{71}$$

Assuming that Ω is *simply connected*, we introduce:

$$\begin{aligned} \mathbf{u} &= \{u_1, u_2\} = \{\partial\psi/\partial x_2, -\partial\psi/\partial x_1\}, \\ \mathbf{v} &= \{v_1, v_2\} = \{\partial\varphi/\partial x_2, -\partial\varphi/\partial x_1\}, \\ \omega &= \partial u_2/\partial x_1 - \partial u_1/\partial x_2, \\ \theta &= \partial v_2/\partial x_1 - \partial v_1/\partial x_2, \\ \mathbf{V}_g &= \{\mathbf{v} \mid \mathbf{v} \in (H^1(\Omega))^2, \nabla \cdot \mathbf{v} = 0, \mathbf{v} \cdot \mathbf{n} = dg/ds \text{ on } \Gamma\}, \\ \mathbf{V}_0 &= \{\mathbf{v} \mid \mathbf{v} \in (H^1(\Omega))^2, \nabla \cdot \mathbf{v} = 0, \mathbf{v} \cdot \mathbf{n} = 0 \text{ on } \Gamma\}, \\ \mathbf{L} &= \begin{pmatrix} 0 & 1 \\ -1 & 0 \end{pmatrix}. \end{aligned}$$

Above, \mathbf{n} is the unit vector of the outward normal at Γ and s is a counter-clockwise curvilinear abscissa on Γ . The formulation (71) is equivalent to

$$\left\{ \begin{array}{l} \text{Find } \mathbf{u}(t) \in \mathbf{V}_g \text{ for all } t > 0 \text{ such that} \\ \int_{\Omega} \partial\omega/\partial t \theta \, dx + \int_{\Omega} \nabla \mathbf{u} : \nabla \mathbf{v} \, dx = \int_{\Omega} \mathbf{Lp} : \nabla \mathbf{v} \, dx, \quad \forall \mathbf{v} \in \mathbf{V}_0, \\ \partial \mathbf{p}/\partial t + \mathbf{p} + \partial I_{\mathbf{Q}_f}(\mathbf{p}) + \mathbf{L} \nabla \mathbf{u} = 0, \\ \{\mathbf{u}(0), \mathbf{p}(0), \omega(0)\} = \{\mathbf{u}_0, \mathbf{p}_0, \omega_0\}. \end{array} \right. \quad (72)$$

The problem (72) has a *visco-elasticity* flavor, $-\mathbf{Lp}$ playing here the role of the so-called *extra-stress tensor*. As $t \rightarrow +\infty$, we obtain thus at the limit a (kind of) *viscosity solution*.

Acknowledgement. The authors would like to thank J. D. Benamou, Y. Brenier, L. A. Caffarelli and P.-L. Lions for assistance and helpful comments and suggestions. The support of NSF (grant DMS-0412267) is also acknowledged.

References

- [Aub82] Th. Aubin. *Nonlinear Analysis on Manifolds, Monge–Ampère Equations*. Springer-Verlag, Berlin, 1982.
- [Aub98] Th. Aubin. *Some Nonlinear Problems in Riemannian Geometry*. Springer-Verlag, Berlin, 1998.
- [BB00] J.-D. Benamou and Y. Brenier. A computational fluid mechanics solution to the Monge–Kantorovich mass transfer problem. *Numer. Math.*, 84(3):375–393, 2000.
- [Cab02] X. Cabré. Topics in regularity and qualitative properties of solutions of nonlinear elliptic equations. *Discrete Contin. Dyn. Syst.*, 8(2):331–359, 2002.
- [CC95] L. A. Caffarelli and X. Cabré. *Fully Nonlinear Elliptic Equations*. American Mathematical Society, Providence, RI, 1995.
- [CH89] R. Courant and D. Hilbert. *Methods of Mathematical Physics, Vol. II*. Wiley Interscience, New York, 1989.

- [CIL92] M. G. Crandall, H. Ishii, and P.-L. Lions. User’s guide to viscosity solutions of second order partial differential equations. *Bull. Amer. Math. Soc. (N.S.)*, 27(1):1–67, 1992.
- [CKO99] L. A. Caffarelli, S. A. Kochenkin, and V. I. Oliker. On the numerical solution of reflector design with given far field scattering data. In L. A. Caffarelli and M. Milman, editors, *Monge–Ampère Equation: Application to Geometry and Optimization*, pages 13–32. American Mathematical Society, Providence, RI, 1999.
- [DG03] E. J. Dean and R. Glowinski. Numerical solution of the two-dimensional elliptic Monge–Ampère equation with Dirichlet boundary conditions: an augmented Lagrangian approach. *C. R. Math. Acad. Sci. Paris*, 336(9):779–784, 2003.
- [DG04] E. J. Dean and R. Glowinski. Numerical solution of the two-dimensional elliptic Monge–Ampère equation with Dirichlet boundary conditions: a least-squares approach. *C. R. Math. Acad. Sci. Paris*, 339(12):887–892, 2004.
- [DG05] E. J. Dean and R. Glowinski. On the numerical solution of a two-dimensional Pucci’s equations with Dirichlet boundary conditions: a least-squares approach. *C. R. Math. Acad. Sci. Paris*, 341(6):375–380, 2005.
- [DG06a] E. J. Dean and R. Glowinski. An augmented Lagrangian approach to the numerical solution of the Dirichlet problem for the elliptic Monge–Ampère equation in two dimensions. *Electron. Trans. Numer. Anal.*, 22:71–96, 2006.
- [DG06b] E. J. Dean and R. Glowinski. Numerical methods for fully nonlinear elliptic equations of the Monge–Ampère type. *Comput. Methods Appl. Mech. Engrg.*, 195(13–16):1344–1386, 2006.
- [DGP91] E. J. Dean, R. Glowinski, and O. Pironneau. Iterative solution of the stream function-vorticity formulation of the Stokes problem. Applications to the numerical simulation of incompressible viscous flow. *Comput. Methods Appl. Mech. Engrg.*, 87(2–3):117–155, 1991.
- [DS96] J. E. Dennis and R. Schnabel. *Numerical Methods for Unconstrained Optimization and Nonlinear Equations*. SIAM, Philadelphia, PA, 1996.
- [Glo84] R. Glowinski. *Numerical Methods for Nonlinear Variational Problems*. Springer-Verlag, New York, 1984.
- [Glo03] R. Glowinski. Finite element methods for incompressible viscous flow. In P. G. Ciarlet and J.-L. Lions, editors, *Handbook of Numerical Analysis, Vol. IX*, pages 3–1176. North-Holland, Amsterdam, 2003.
- [GP79] R. Glowinski and O. Pironneau. Numerical methods for the first biharmonic equation and for the two-dimensional Stokes problem. *SIAM Rev.*, 17(2):167–212, 1979.
- [GT01] D. Gilbarg and N. Trudinger. *Elliptic Partial Differential Equations of Second Order*. Springer-Verlag, Berlin, 2001.
- [Jan88] R. Jansen. The maximum principle for viscosity solutions of fully nonlinear second order partial differential equations. *Arch. Rational Mech. Anal.*, 101:1–27, 1988.
- [OP88] V. I. Oliker and L. D. Prussner. On the numerical solution of the equation $(\partial^2 z / \partial x^2)(\partial^2 z / \partial y^2) - ((\partial^2 z / \partial x \partial y))^2 = f$ and its discretization, I. *Numer. Math.*, 54(3):271–293, 1988.
- [Pir89] O. Pironneau. *Finite Element Methods for Fluids*. Wiley, Chichester, 1989.
- [Urb88] J. I. E. Urbas. Regularity of generalized solutions of Monge–Ampère equations. *Math. Z.*, 197(3):365–393, 1988.